Field Observations on Modal Properties of a Tall Building

Zuo Zhu
PhD student, School of Engineering, University of Liverpool, Liverpool, UK

Siu-Kui Au
Professor, School of Engineering, University of Liverpool, Liverpool, UK

ABSTRACT: This paper presents field observations on the modal properties of a tall building under ambient conditions. Acceleration data was collected by a force-balance triaxial accelerometer at one corner of the building. It was divided into non-overlapping time windows to investigate the amplitude dependence of natural frequencies and damping ratios. Four modes were identified by Bayesian Operational Modal Analysis (BAYOMA) where the first two modes are closely-spaced while the others are well-separated. The results show that there is an inverse trend between the natural frequencies and modal root-mean-square value (RMS) while the damping ratios show a positive correlation with the modal RMS.

1. INTRODUCTION

The characterisation of dynamic properties of structures plays an important role in assessing their response subjected to dynamic loads possibly due to earthquakes, traffic, human activities, strong wind, etc. At the design stage, the natural frequencies and mode shapes can be assessed based on a finite element model incorporating structural information. Damping characteristics are usually assumed via classical damping ratios since there is no widely accepted mechanistic model. The finite element model only reflects the structures under idealised conditions. The assumed damping ratios could be far from the actual value even if the structure behaves as classically damped. On the other hand, modal properties can be affected by many factors, such as vibration amplitude and temperature (Cross et al. 2013; Tamura et al. 1996; Zhang et al. 2016). Such effects cannot be captured in the computer model. In the above context, in-situ vibration testing provides an effective means for accessing the actual dynamic properties of a constructed structure.

Operational modal analysis (OMA), also known as ambient modal identification, aims at identifying the natural frequencies, damping ratios and mode shapes of a constructed structure using the ambient vibration data (Brincker and Ventura 2015; Ewins 2000; Au 2017). It can be conducted economically without knowing the specific information of loading, which is assumed to be statistically random. Bayesian approach offers a fundamental means for OMA consistent with structural dynamics and probability modelling assumptions. In addition to the 'most probable value' which is akin to the 'best' or 'optimal' estimate in non-Bayesian methods, it also assesses the identification uncertainty via the posterior covariance matrix. Mathematical formulation in the frequency domain first appeared in Yuen and Katafygiotis (2003). Later fast algorithms that allow for practical applications were developed in different contexts, e.g., well-separated modes (Au 2011), closely-spaced modes (Au 2012a, 2012b). These are collectively referred as Bayesian Operational Modal Analysis (BAYOMA). Recent applications can be found in Brownjohn et al. (2018), Hu et al. (2018), Lam et al. (2017), Liu et al. (2016), etc.

This paper presents work on field observations on the modal properties of a tall building identified using ambient acceleration

data with Bayesian OMA. The amplitude dependence of the natural frequencies and damping ratios are investigated.

2. FIELD BUILDING

The structure investigated in this work is a tall office building. It has eighteen stories with a total height of 65 m. The shape of the plan is rectangular spanning over a 20 m × 125 m area. In order to monitor the ambient vibration of the structure, a force-balance triaxial accelerometer paired with a 24bit data logger was deployed at the southwest corner on the 12/F. The noise level of the accelerometer is around $0.1\ \mu g/\sqrt{\text{Hz}}$. Long term monitoring data was collected at a sampling rate of 50 Hz. The study here considers data spanning over eight days in winter. It is divided into 15-min non-overlapping time windows (total 768 sets). The primary interest is to investigate how the modal properties vary with the amplitude of the vibration. Figure 1 shows the acceleration time history of a typical dataset.

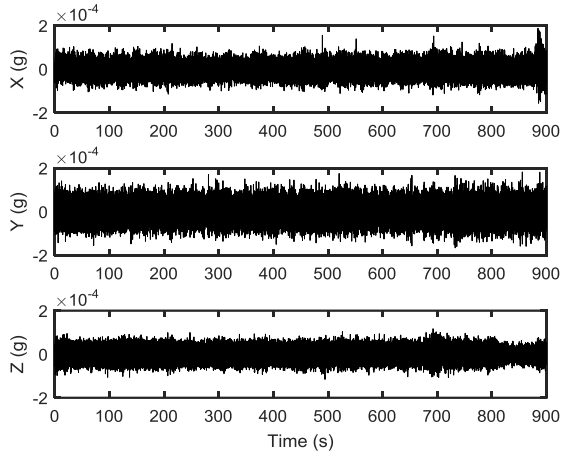

Figure 1 Time history of a typical set of acceleration data

3. BAYESIAN MODAL IDENTIFICATION

BAYOMA is applied to identify the modal properties and quantify the associated identification uncertainties. The theory is briefly introduced in this section. Let $\left\{\hat{\ddot{\mathbf{x}}}_j\right\}_{j=0}^{N-1}(n\times 1)$ be the measured acceleration data at *n* DOFs (degrees of freedom), where *N* is the number of samples per channel. It is modelled as

$$\hat{\ddot{\mathbf{x}}}_j = \ddot{\mathbf{x}}_j + \boldsymbol{\varepsilon}_j \tag{1}$$

where $\ddot{\mathbf{x}}_j$ is the theoretical model acceleration that depends on the set of modal parameters $\boldsymbol{\theta}$; $\boldsymbol{\varepsilon}_j$ is the prediction error accounting for the modelling error and instrument noise. The scaled one-sided FFT (Fast Fourier Transform) of $\hat{\ddot{\mathbf{x}}}_j$ at frequency $f_k = k/N\Delta t$ (Hz) is defined as

$$F_k = \sqrt{\frac{2\Delta t}{N}}\sum_{j=0}^{N-1}\hat{\ddot{\mathbf{x}}}_j e^{-2\pi \mathbf{i} jk/N} \tag{2}$$

where Δt (sec) is the sampling time interval and $\mathbf{i}^2=-1$; $k=1,\cdots,N_q$ with $N_q=\text{int}\left[N/2\right]+1$ (int[·] denotes the integer part) being the index corresponding to the Nyquist frequency. Typically, only the F_k within a selected band covering the mode of interest is used for modal identification.

The set of modal parameters to be identified, $\boldsymbol{\theta}$, consists of the natural frequencies $\{f_i\}_{i=1}^m$, damping ratios $\{\zeta_i\}_{i=1}^m$, modal force PSD (power spectral density) matrix $\mathbf{S}\in R^{m\times m}$, prediction error PSD S_e and mode shape matrix $\boldsymbol{\Phi}=\left[\boldsymbol{\varphi}_1,\boldsymbol{\varphi}_2,\cdots,\boldsymbol{\varphi}_m\right]\in R^{n\times m}$, where m is the number of modes in the selected band and $\boldsymbol{\varphi}_i\ (i=1,\cdots,m)$ is the *i-th* mode shape confined to the measured DOFs. Using Bayes' theorem, the posterior PDF given the measured data is given by

$$p\left(\boldsymbol{\theta}\middle|\{F_k\}\right)=p\left(\{F_k\}\right)^{-1}p\left(\{F_k\}\middle|\boldsymbol{\theta}\right)p(\boldsymbol{\theta}) \tag{3}$$

where $p\left(\{F_k\}\right)^{-1}$ is a normalising constant. For long data the prior PDF $p(\boldsymbol{\theta})$ is a slowly varying function of $\boldsymbol{\theta}$ compared to the likelihood function $p\left(\{F_k\}\middle|\boldsymbol{\theta}\right)$ and thus can be assumed to be a uniform distribution. The posterior PDF is then proportional to the likelihood function:

$$p\left(\boldsymbol{\theta}\middle|\{F_k\}\right)\propto p\left(\{F_k\}\middle|\boldsymbol{\theta}\right) \tag{4}$$

For long data, the FFT vectors $\{F_k\}$ follow a (circular symmetric) complex Gaussian

distribution and are independent at different frequencies. Consequently, one has,

$$p\left(\{F_k\}\middle|\boldsymbol{\theta}\right)=\prod_k p\left(F_k\middle|\boldsymbol{\theta}\right) \tag{5}$$

where the product is taken over all the frequencies within the selected band;

$$p\left(F_k\middle|\boldsymbol{\theta}\right)=\frac{\pi^{-n}}{\left|\mathbf{E}_k\left(\boldsymbol{\theta}\right)\right|}\exp\left[-F_k^*\mathbf{E}_k\left(\boldsymbol{\theta}\right)^{-1}F_k\right] \tag{6}$$

and $\mathbf{E}_k\left(\boldsymbol{\theta}\right)=E\left[F_k\,F_k^*\middle|\boldsymbol{\theta}\right]$ is the theoretical PSD matrix for given $\boldsymbol{\theta}$. Suppose that the prediction errors at different measured DOFs are i.i.d. (independent and identically distributed) with PSD S_e and that they are also independent of the modal force. Then

$$\mathbf{E}_k=\boldsymbol{\Phi}\mathbf{H}_k\boldsymbol{\Phi}^T+S_e\mathbf{I}_n \tag{7}$$

where $\mathbf{I}_n\in R^n$ is the identity matrix; the (i, j)-entry of $\mathbf{H}_k$ is given by

$$\begin{aligned}\mathbf{H}_k\left(i,j\right)=S_{ij}&\left[1-\beta_{ik}^2+2\zeta_i\beta_{ik}\mathbf{i}\right]^{-1}\\&\times\left[1-\beta_{jk}^2-2\zeta_j\beta_{jk}\mathbf{i}\right]^{-1}\end{aligned} \tag{8}$$

and $\beta_{ik}=f_i/f_k$; f_i is the natural frequency of the *i-th* mode; S_{ij} is the cross spectral density between the *i-th* and *j-th* modal force.

It is more convenient to work with the negative log-likelihood function (NLLF) for analysis and computation. Eq. (4) can be rewritten as

$$p\left(\boldsymbol{\theta}\middle|\{F_k\}\right)\propto p\left(\{F_k\}\middle|\boldsymbol{\theta}\right)=e^{-L(\boldsymbol{\theta})} \tag{9}$$

Combining Eq.(5), Eq.(6) and Eq.(9), one can obtain

$$\begin{aligned}L\left(\boldsymbol{\theta}\right)=nN_f\ln\pi+\sum_k\ln\left|\mathbf{E}_k\left(\boldsymbol{\theta}\right)\right|\\+\sum_k F_k^*\mathbf{E}_k\left(\boldsymbol{\theta}\right)^{-1}F_k\end{aligned} \tag{10}$$

where N_f is the number of frequency ordinates within the selected band.

Based on Eq.(10), the most probable value (MPV) of the modal parameters can be determined by minimising the NLLF function $L\left(\boldsymbol{\theta}\right)$. Approximating the NLLF at the MPV by a second order Taylor series leads to a Gaussian approximation of the posterior PDF. It can be shown that the posterior covariance matrix is equal to the inverse of the Hessian of the NLLF at the MPV.

In applications, determining the MPV by directly minimising the original NLLF function Eq.(10) is impractical since $\mathbf{E}_k\left(\boldsymbol{\theta}\right)$ is close to singular and the computational time increases dramatically with the number of measured DOFs. Fast algorithms have been developed (Au 2011, 2012a, 2012b) and they are used in this paper to identify the modal parameters.

4. ANALYSIS RESULTS

We first present the analysis of a typical time window of data (see Figure 1). The same procedure is then used for all time windows to investigate potential amplitude dependence of the modal parameters. Figure 2 shows the root PSD of a typical time window of data. The blue, red and yellow lines respectively show the measured data along the x, y and z direction. Figure 3 shows the corresponding singular value spectrum. The number of lines significantly above the remaining ones indicates the number of modes. Four modes are evident in the spectrum below 2.5 Hz. The first two modes are closely-spaced while the others are well-separated. The prefixes 'TX', 'TY' and 'R' in Figure 3 stand for *x*-, *y*- and torsional modes of the building. The hand-picked initial guesses and the frequency bands are respectively shown with a circle and the symbol '[-]'.

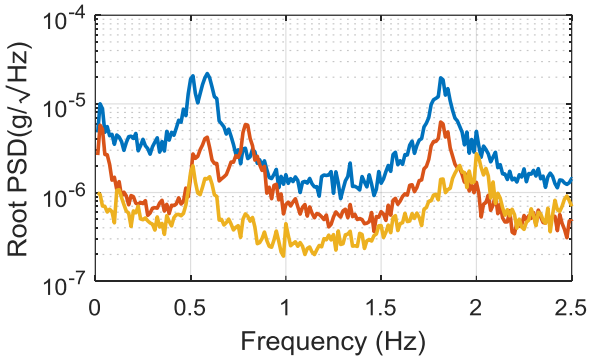

Figure 2 Root power spectral density, 15-min data

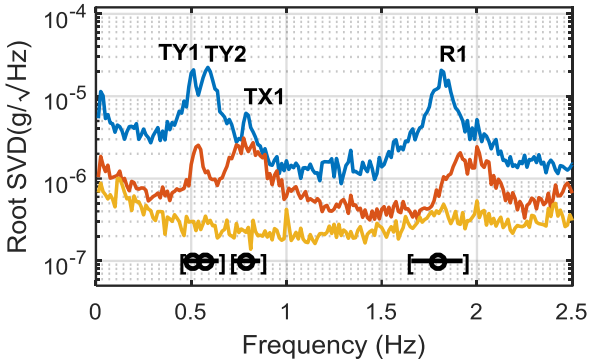

Figure 3 Root singular value, 15-min data

Table 1 summarises the identified modal properties. The columns under 'MPV' show the identified most probable value while the columns under 'c.o.v' show the coefficient of variation (= standard deviation/MPV), which reflects the identification precision of the subject parameter given the information in the data and interpreted consistent with modelling assumptions and probability theory. The posterior c.o.v. of natural frequencies are all less than 1%, which are much lower than those of damping ratios. The latter are in the order of a few tens of percent. Generally the uncertainty of the damping ratio is the highest compared to other modal parameters. The c.o.v. of the damping ratio in the third mode is higher than those in the other modes. This can be reasoned from Figure 3 where the signal-to-noise ratio (SNR) of the third mode is much lower than those of others. The relationship between identification uncertainty and SNR can be fundamentally explained based on recent discovery on 'uncertainty laws'. Details are referred to Au et. al (2018).

Table 1: Summary of identified modal properties.

Mode	*f*		*ζ*	
	MPV (Hz)	*c.o.v. (%)*	*MPV (%)*	*c.o.v. (%)*
1	*0.512*	*0.33*	*2.48*	*14.44*
2	*0.574*	*0.59*	*5.36*	*12.33*
3	*0.791*	*0.33*	*1.89*	*20.45*
4	*1.817*	*0.15*	*1.53*	*11.32*

We next investigate the relationship between the modal properties and vibration amplitude. Based on the identified values of the modal parameters from different segments, the modal acceleration RMS (root-mean-square) is calculated by Eq. (11) as a proxy for quantifying the vibration amplitude (Au 2012c).

$$R_i = \sqrt{\frac{\pi f_i S_{ii}}{4\zeta_i}} \tag{11}$$

where S_{ii} denotes the modal force PSD of the *i-th* mode .

Figure 4 shows how the natural frequencies and damping ratios vary with the vibration amplitude, where the result is plotted with a dot at the MPV and an error bar indicating ±1 (posterior) standard deviation. The modal RMS ranges from micro-g to 100 micro-g. The variability of the modal parameters is significantly larger than the posterior uncertainty, which suggests that the trends are statistically significant.

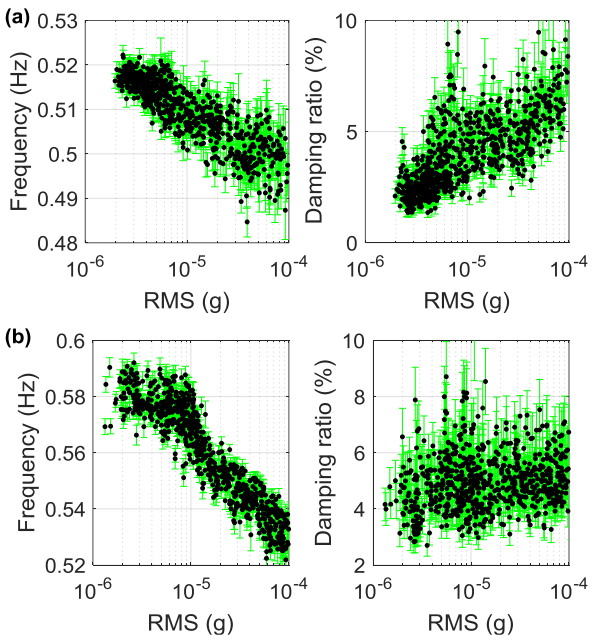

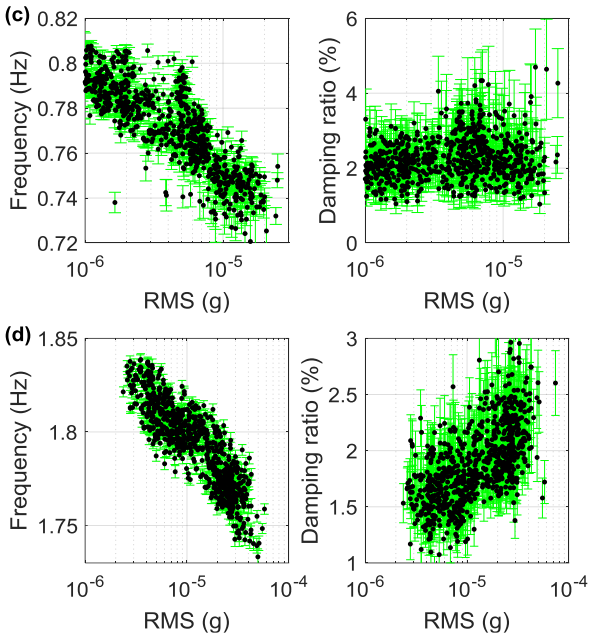

Figure 4 Identified natural frequencies and damping ratios vs modal RMS (a) Mode 1, (b) Mode 2, (c) Mode 3, (d) Mode 4

The plots on the left columns in Figure 4 suggest that the natural frequencies show a decreasing trend with the modal RMS, regardless of mode. They decrease by around 6%, 10%, 9% and 5% for Mode 1 to Mode 4, respectively. From the figures on the right columns, it seems that the damping ratio of the third mode is insensitive to the modal RMS. Nevertheless, it is apparent that the values of the first mode and the forth mode increase with the modal RMS. For high RMS the identified damping ratios of the first mode were in excess of 5% which is not typical. Efforts have been made to investigate if this is merely due to analysis or instrumentation flaws, although no peculiarity has been found so far. The identified damping ratio of the second mode does not show a strong amplitude dependence.

5. CONCLUSIONS

This work presents the field observations on the modal properties of a tall building identified by Bayesian Operational Modal Analysis. Viewing amplitude dependence via the most probable values together with error bars showing identification uncertainty helps one delineate potential systematic trend from scattering due to lack of information. As remark, similar negative correlation of frequency and positive correlation of damping ratios with the modal RMS have been observed in many previous studies, e.g., Au et al. (2012c), Li et al. (2003) and Satake et al. (2003).

6. REFERENCES

Au, S. K. (2011). Fast Bayesian FFT method for ambient modal identification with separated modes. Journal of Engineering Mechanics, 137(3), 214-226.

Au, S. K. (2012a). Fast Bayesian ambient modal identification in the frequency domain, Part I: Posterior most probable value. Mechanical Systems and Signal Processing, 26, 60-75.

Au, S. K. (2012b). Fast Bayesian ambient modal identification in the frequency domain, Part II: posterior uncertainty. Mechanical Systems and Signal Processing, 26, 76-90.

Au, S. K., Zhang, F. L., & To, P. (2012c). Field observations on modal properties of two tall buildings under strong wind. Journal of Wind Engineering and Industrial Aerodynamics, 101, 12-23.

Au, S. K. (2017). Operational Modal Analysis: Modeling, Bayesian Inference, Uncertainty Laws. Springer.

Au, S. K., Brownjohn, J. M., & Mottershead, J. E. (2018). Quantifying and managing uncertainty in operational modal analysis. Mechanical Systems and Signal Processing, 102, 139-157.

Brincker, R., & Ventura, C. (2015). Introduction to operational modal analysis. John Wiley & Sons.

Brownjohn, J. M. W., Au, S. K., Zhu, Y., Sun, Z., Li, B., Bassitt, J., ... & Sun, H. (2018). Bayesian operational modal analysis of Jiangyin Yangtze River Bridge. Mechanical Systems and Signal Processing, 110, 210-230.

Cross, E. J., Koo, K. Y., Brownjohn, J. M. W., & Worden, K. (2013). Long-term monitoring and data analysis of the Tamar Bridge. Mechanical Systems and Signal Processing, 35(1-2), 16-34.

Ewins, D. J. (2000). Modal testing: theory, practice and application (mechanical engineering research studies: engineering dynamics series). Research studies Pre, 2nd ed., ISBN-13, 978-0863802188.

Hu, Y. J., Guo, W. G., Jiang, C., Zhou, Y. L., & Zhu, W. (2018). Looseness localization for bolted joints using Bayesian operational modal

analysis and modal strain energy. Advances in Mechanical Engineering, 10(11), 1-10.

Lam, H. F., Zhang, F. L., Ni, Y. C., & Hu, J. (2017). Operational modal identification of a boat-shaped building by a Bayesian approach. Engineering Structures, 138, 381-393.

Li, Q. S., Yang, K., Wong, C. K., & Jeary, A. P. (2003). The effect of amplitude-dependent damping on wind-induced vibrations of a super tall building. Journal of Wind Engineering and Industrial Aerodynamics, 91(9), 1175-1198.

Liu, P., Zhang, F. L., & Lian, P. Y. (2016). Dynamic characteristic analysis of two adjacent multi-grid composite wall structures with a seismic joint by a Bayesian approach. Journal of Earthquake Engineering, 20(8), 1295-1321.

Satake, N., Suda, K. I., Arakawa, T., Sasaki, A., & Tamura, Y. (2003). Damping evaluation using full-scale data of buildings in Japan. Journal of structural engineering, 129(4), 470-477.

Tamura, Y., & Suganuma, S. Y. (1996). Evaluation of amplitude-dependent damping and natural frequency of buildings during strong winds. Journal of wind engineering and industrial aerodynamics, 59(2-3), 115-130.

Yuen, K. V., & Katafygiotis, L. S. (2003). Bayesian fast Fourier transform approach for modal updating using ambient data. Advances in Structural Engineering, 6(2), 81-95.

Zhang, F. L., Xiong, H. B., Shi, W. X., & Ou, X. (2016). Structural health monitoring of Shanghai Tower during different stages using a Bayesian approach. Structural Control and Health Monitoring, 23(11), 1366-1384.